Fat-suppression MR imaging of the orbit.

J Simon, J Szumowski, S Totterman, D Kido, S Ekholm, A Wicks and D Plewes

AJNR Am J Neuroradiol 1988, 9 (5) 961-968
http://www.ajnr.org/content/9/5/961

Fat-Suppression MR Imaging of the Orbit

J. Simon[1]
J. Szumowski
S. Totterman
D. Kido
S. Ekholm
A. Wicks
D. Plewes

The effect of fat suppression on orbital MR imaging was tested by using a derivative of the Dixon method called chopper fat suppression in eight normal volunteers and eight patients with normal conventional orbital MR studies. Chopper fat suppression requires no postacquisition image processing or increased scan time and can be applied through a wide range of T1 to T2 weighting. In normal orbits, fat suppression was found to be advantageous for imaging the lacrimal gland and the optic nerve. Using fat-suppressed T1- or intermediate-weighted sequences, 2000/30 (TR/TE), the optic nerve was recognized by its high signal intensity relative to adjacent CSF, dural sheath, and surrounding fat. The technique minimized loss of anatomic detail by reducing chemical shift misregistration artifact. Disadvantages included an overall lower orbital signal/noise ratio.

When used in conjunction with a TR/TE combination carefully selected for both anatomic region of interest and suspected pathology, the fat-suppression technique has the potential for improving the visualization of orbital lesions.

High-resolution MR imaging of the orbit with surface-coil techniques has resulted in excellent anatomic detail [1], which is competitive with high-resolution CT [2–4]. Orbital detail seen via MR imaging is, like CT, largely the result of tissue contrast made possible by the inherent high orbital fat content. However, most conventional orbital MR imaging strategies have some limitations related to fat. These can be broadly divided into two categories: limitations due to loss of anatomic detail as a result of chemical shift misregistration artifact [5] and contrast-related limitations.

To minimize some of these visualization difficulties in the orbit and other regions, techniques have been introduced to suppress the signal from lipid. These include the Dixon method [6], which has recently been applied to imaging the optic nerve [5] and orbital lesions [7]; short inversion time inversion recovery (STIR) sequences [8] applied to studies of optic neuritis [9]; and chemical shift selective (CHESS) imaging [10]. The present study was designed to test a recently developed fat-suppression technique that is based on a simple modification of Dixon's method. This technique, known as chopper fat suppression [11], requires only software modification. Chopper fat suppression is clinically attractive since it allows for strong lipid suppression yet requires no postacquisition image reconstruction or manipulation, no increased scan time, and can be applied through a wide range of T1 to T2 weighting.

We have evaluated this technique through a range of echo delay time (TE) and repetition time (TR) combinations to determine its feasibility and to develop an approach for applying the technique to pathologic orbital MR studies.

Materials and Methods

All studies were performed on a GE Signa MR system operating at 1.5 T, with a round 5-in. diameter surface coil as receiver. The studies were performed with the surface coil

Received June 18, 1987; accepted after revision January 29, 1988.

Presented at the annual meeting of the American Society of Neuroradiology, New York, May 1987.

[1] All authors: Department of Radiology, Box 694, University of Rochester Medical Center, Rochester, NY 14642. Address reprint requests to J. H. Simon.

AJNR 9:961–968, September/October 1988
0195–6108/88/0905–0961

centered over both orbits, just above the skin surface, with the patient supine. Imaging sequences with variable TR and TE were obtained with a 16-cm field of view. Section thickness was 3 mm for axial images and 5 mm for coronal images, using two excitations, a 128 × 256 matrix, and other parameters varied as indicated. The results are based on examination of eight normal volunteers and eight patients with normal conventional orbital MR studies.

The fat-suppression technique uses to advantage the fact that typically MR images are acquired with two excitations to improve signal-to-noise ratio and to compensate for DC effect and 180° pulse imperfections in spin-echo images. The phase of the 90° excitation pulse in the second acquisition is reversed relative to the phase in the first pulse. Two data sets are then subtracted and the image is formed after phase-encoding steps are completed. The process of paired excitations is frequently referred to as "chopper" sequencing by the manufacturer.* Chopper fat suppression is compared with the original (magnitude) Dixon method [6] in Figure 1. In chopper fat suppression the first scan is the usual acquisition and creates a raw data set with fat and water magnetization oriented parallel. In the second excitation, the phase of the 90° pulse is reversed and a shift is introduced in the position of the 180° pulse, resulting in a raw data set in which fat and water magnetization are antiparallel. The two sets of raw data are subsequently subtracted as part of the acquisition process. If the experiment is performed with the excitation frequency centered on the water resonance, the procedure leads to automatic fat suppression from the image.

* General Electric, Milwaukee, WI.

Multiple studies in two normal volunteers, ages 36 and 37 years, respectively, were used to evaluate the effect of fat suppression on normal orbit anatomy. Eight sets of data were obtained, each of which included consecutively acquired images by conventional and fat-suppression techniques at similar locations in the axial and coronal planes. There was no attempt to repeat the studies to obtain optimal examinations since the purpose of this phase of the study was, in part, to evaluate the reproducibility of the technique. The studies were subsequently reviewed by five radiologists. Each reviewer compared the fat-suppressed images with the the conventionally obtained paired images at the same TR and TE combination. Each pair of images was scored on a 5-point scale for eight separate anatomic regions of interest. The rating system designated a score of 0 when both acquisitions provided essentially equivalent information. A score of +1 or −1 was given when the fat-suppressed image was, overall, more or less acceptable than the conventional image, respectively, but the difference was not marked. A score of +2 or −2 was entered when there was a marked difference in the images, favorable or unfavorable for fat suppression, respectively. There was no attempt to blind reviewers to the sequence they were evaluating since the basis of the image (fat-suppressed versus conventional) was usually obvious when both pairs were simultaneously presented.

Results

T1-Weighted Images

On conventional T1-weighted images, 400–600/25–40/2 (TR range/TE range/excitations), orbital fat was the primary

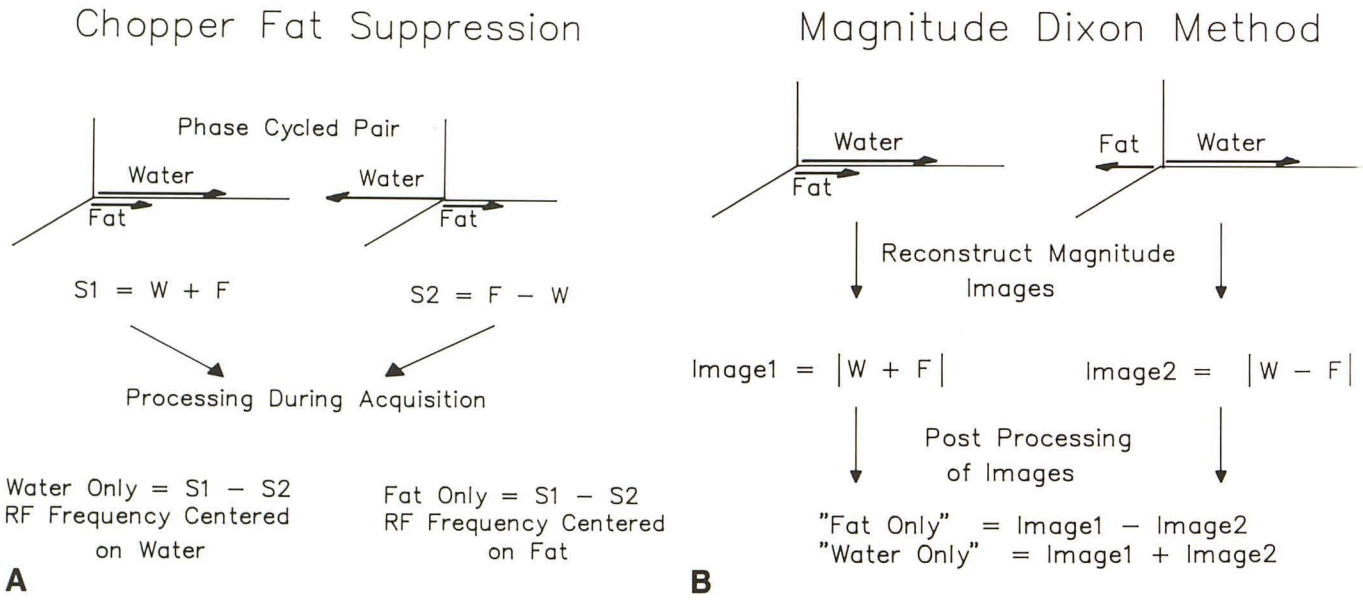

Fig. 1.—*A* and *B*, Chopper fat suppression (*A*) compared with magnitude Dixon method (*B*). In the chopper fat-suppression technique, the first raw data set (S1) is acquired with the fat and water magnetization oriented parallel, such that signal intensity is based on the sum of water (W) plus fat (F). In the second raw data set (S2), owing to a shift in the position of the 180° pulse, the fat and water magnetization are antiparallel, and signal intensity is the result of fat minus water. The two raw data sets are subtracted (S1 − S2) as part of the acquisition process, resulting in a water-only image when the excitation frequency is centered on the water resonance. Image intensity will be directly proportional to water content per voxel (W + F − F + W) = 2W. Averaged value (2W/2) = W. When the excitation frequency is centered on the fat resonance, S2 = W − F and the procedure results in a fat-only image. In the original (magnitude) Dixon method, separate water-plus-fat and water-minus-fat images are acquired, each image based on the magnitude (absolute value) of the magnetization parallel W + F or antiparallel W − F. These images are subsequently postprocessed to obtain water-only images (image 1 + image 2). Note that in voxels dominated by fat (such as the orbit), the magnitude calculation can result in a signal intensity that does not reflect water per voxel but rather still reflects fat content [11]. For example, in image 2, when fat dominates, W − F will be negative and therefore the magnitude of W − F will equal F − W, resulting in a fat-only image (W + F + F − W) = 2F. Averaged value ($\frac{2F}{2}$) = F.

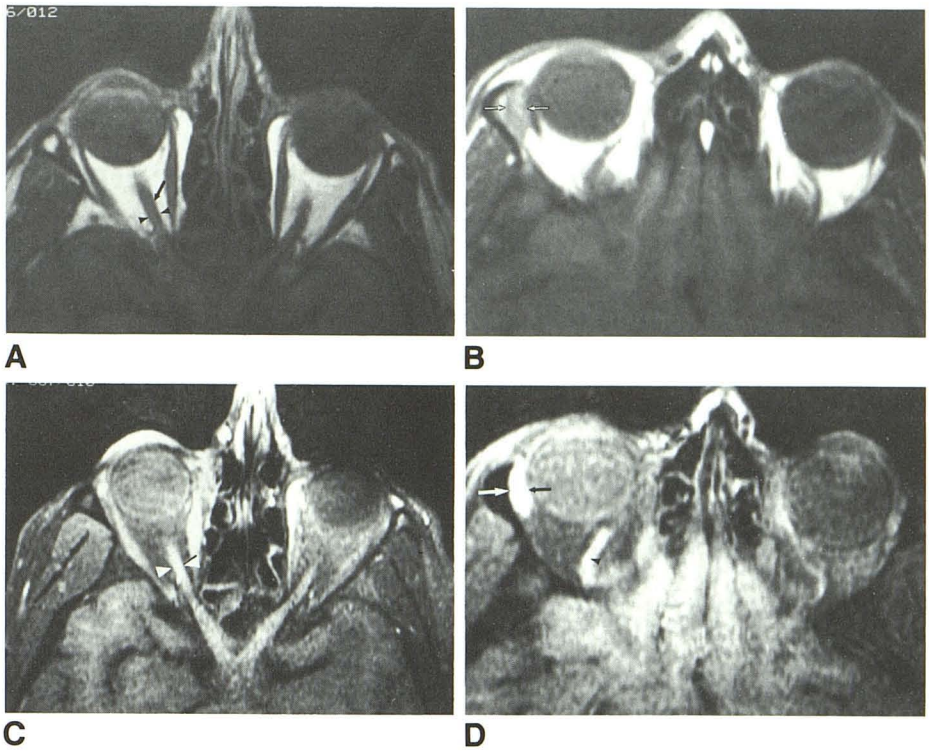

Fig. 2.—Conventional T1-weighted images of the orbit (*A* and *B*) compared with fat-suppressed images (*C* and *D*) in a normal subject. Axial 3-mm-thick images (400/25) with a 128 × 256 matrix, contiguous slices with a 16-cm field of view. Acquisition time 3 min, 27 sec.

***A*, On this conventional image fat envelopes multiple low-intensity structures, including a low-intensity stripe caused by chemical shift artifact (*arrow*), CSF, optic nerve, and dural sheath, creating the illusion of a thicker nerve (between *arrowheads*).**

***B*, On this conventional image the lacrimal gland (between *arrows*) lies adjacent to muscle, orbital and intramedullary fat, and bone.**

***C*, On this fat-suppressed image, the optic nerve alone (between *arrowheads*) is highlighted against surrounding low-intensity CSF, dural sheath, and fat, and there is loss of chemical shift artifact.**

***D*, On this fat-suppressed image, the superior ophthalmic vein (*arrowhead*) has become hyperintense relative to neighboring fat. With fat suppression, lacrimal gland contrast is increased (between *arrows*).**

factor accounting for structural detail (Figs. 2A and 2B). For example, high signal intensity from fat outlined the optic nerve sheath and extraocular muscle sheaths, the posterior limits of the globe, and the orbital veins. With the exception of the lacrimal gland, which was not well contrasted with fat, the signal intensity ratio for most structures/fat was low. T1-weighted images were reproducibly of high quality for evaluating most major anatomic features, primarily because of the high contrast/noise ratio.

A more detailed evaluation of fine orbital anatomy, however, showed potential weaknesses of conventional T1-weighted techniques. For example, the dominant high signal intensity of fat interfered with visualization of the optic nerve, distinct from investing CSF and dural sheath. The margins of the intracanalicular segment of the optic nerve were often indistinct because of adjacent high signal intensities presumed to be fat within the marrow of the adjacent bone. Similarly, muscle was visually poorly separated from its fibrous sheath.

The posterior wall of the globe (including sclera, choroid, and retinal layers) contrasted poorly with the adjacent vitreous humor. Within the globe, and unrelated to orbital fat, the lens, ciliary body, and aqueous humor showed a narrow range of contrast and limited fine detail.

In the majority of images, bands of high and low intensity, typical of those described as chemical shift misregistration artifacts, were observed parallel to the long axis of the optic nerve sheath and muscles on the axial images. On coronal images these occurred principally above and below nerve and muscle in accordance with the direction of the frequency-encoding gradient.

Fat suppression applied to similar T1-weighted sequences resulted in considerable variation in signal intensity and modification of anatomic detail compared with conventional images (Figs. 2C and 2D). The signal intensity relationship between optic nerve and fat, lacrimal gland and fat, and muscle and fat reversed with ratios strongly positive with fat suppression. Fat suppression resulted in a more realistic visual representation of the thickness of optic nerve and muscle, presumably the result of increased positive contrast between optic nerve with low-intensity CSF, nerve sheath, and orbital fat; and muscle contrast with low-intensity fibrous sheath and fat. Visualization of lacrimal gland margins was improved by the greater contrast. In addition, chemical shift artifact was decreased and resulted in truer anatomic borders, particularly affecting optic nerve detail when compared with conventional T1-weighted images.

Intermediate-Weighted Images

Conventional intermediate-weighted images (2000/30) (Figs. 3A–3C) were characterized by acceptable orbital anatomy, even with an axial slice thickness of 3 mm. Ratios of signal intensity of optic nerve/fat and muscle/fat remained favorable for high-quality imaging of anatomic features. In addition, independent of fat contrast, tissue contrast resulted in better separation of low-intensity lens from adjacent higher-intensity fluid, and resolution of the globe surface into at least two layers. As on T1-weighted images, we were unable to reliably distinguish optic nerve from surrounding CSF and muscle from surrounding fibrous sheath. Lacrimal gland detail was poor because of its limited contrast with fat, and chemical shift artifact remained a problem.

On fat-suppressed intermediate-weighted images (Figs. 3D–3F), there again was reversal of several important signal-

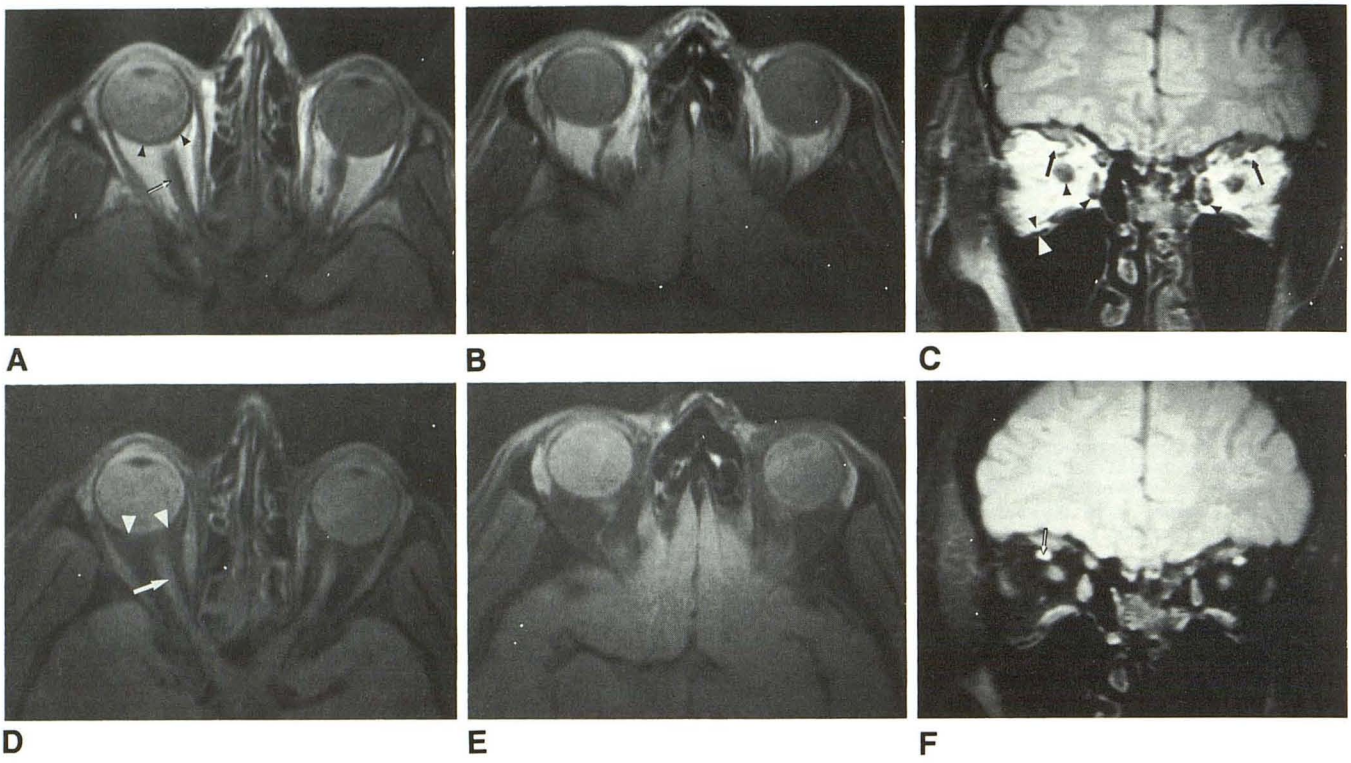

Fig. 3.—*A–F*, Conventional intermediate-weighted images (*A–C*) compared with fat-suppressed images (*D–F*) in a normal subject. Scan parameters are the same as those for Fig. 2, but with 2000/30 and skip 0 slices. Acquisition time 8 min, 38 sec. Note that optic nerve (*arrows* in *A* and *D*) appears thinner and its margins better defined on fat-suppressed image (*D*), particularly in the intracanalicular segment, than on conventional image (*A*). On conventional image, posterior sclera is outlined by fat (*arrowheads* in *A*), but becomes isointense with fat on suppressed image (*arrowheads* in *D*). Same sequence pair at lacrimal gland level (*B* and *E*). Coronal image (*C*) (slice thickness of 5 mm) shows prominent bright and dark bands from chemical shift artifacts, most notable along margins of optic nerve sheath and muscles (*arrowheads*) in this conventional image. Artifacts are decreased on fat-suppressed image (*F*). On coronal images, the superior ophthalmic vein is a high-intensity structure (*arrows* in *C* and *F*), easily defined by its contrast with fat on suppressed image (*F*).

intensity relationships. Contrast between optic nerve or muscle and fat was lower than on conventional images, but the margin of positive contrast was sufficient for good anatomic detail. As on fat-suppressed T1-weighted images, these sequences provided a truer image of optic nerve and muscle thickness, and intracanalicular optic nerve margins were more consistently visible. The lacrimal gland margins were sharply defined, similar to fat-suppressed T1-weighted images. Chemical shift artifact varied from minimal to inapparent.

A potentially unfavorable feature of fat suppression was loss of globe wall detail compared with the conventional sequence. For example, the low-intensity retroorbital fat was nearly isointense with sclera.

T2-Weighted Images

Conventional T2-weighted images (2000/60) provided favorable anatomic detail for anterior chamber structures and the globe surface because of the relative high intensity of intraocular fluids (Fig. 4A). Lacrimal gland contrast with surrounding fat increased to more positive levels (Fig. 4B) with improved margin detail compared with intermediate- and T1-weighted images.

In the retroorbit, fat decreased to near isointensity with optic nerve, which resulted in less favorable contrast on both the axial (Fig. 4A) and coronal (Fig. 4C) images. The image distortion effect of chemical shift artifact visually increased and resulted in major loss of anatomic detail. Our preliminary experience with conventional images obtained with greater T2 weighting (TE = 90) suggests some gain in contrast between tissues of interest, but with decreased signal to noise and prominent chemical shift artifact obscuring details.

Fat-suppressed T2-weighted images showed more favorable signal intensity ratios for visualization of optic nerve, muscle (Figs. 4D and 4F), and lacrimal gland (Fig. 4E). Although there was some decrease in signal to noise compared with the 2000/30 images, in most cases diagnostic quality was thought to be good. Similar to the intermediate- and T1-weighted images, and compared with conventional techniques, intracanalicular optic nerve detail was improved in most studies. CSF was not usually recognized as a distinct entity from nerve, contributing to loss of advantage of the positive optic nerve/fat signal ratio.

Figure 5 shows the average evaluation scores for eight anatomic regions of interest at various combinations of TR and TE used to generate T1-, intermediate-, and T2-weighted images. Several anatomic regions were imaged to advantage

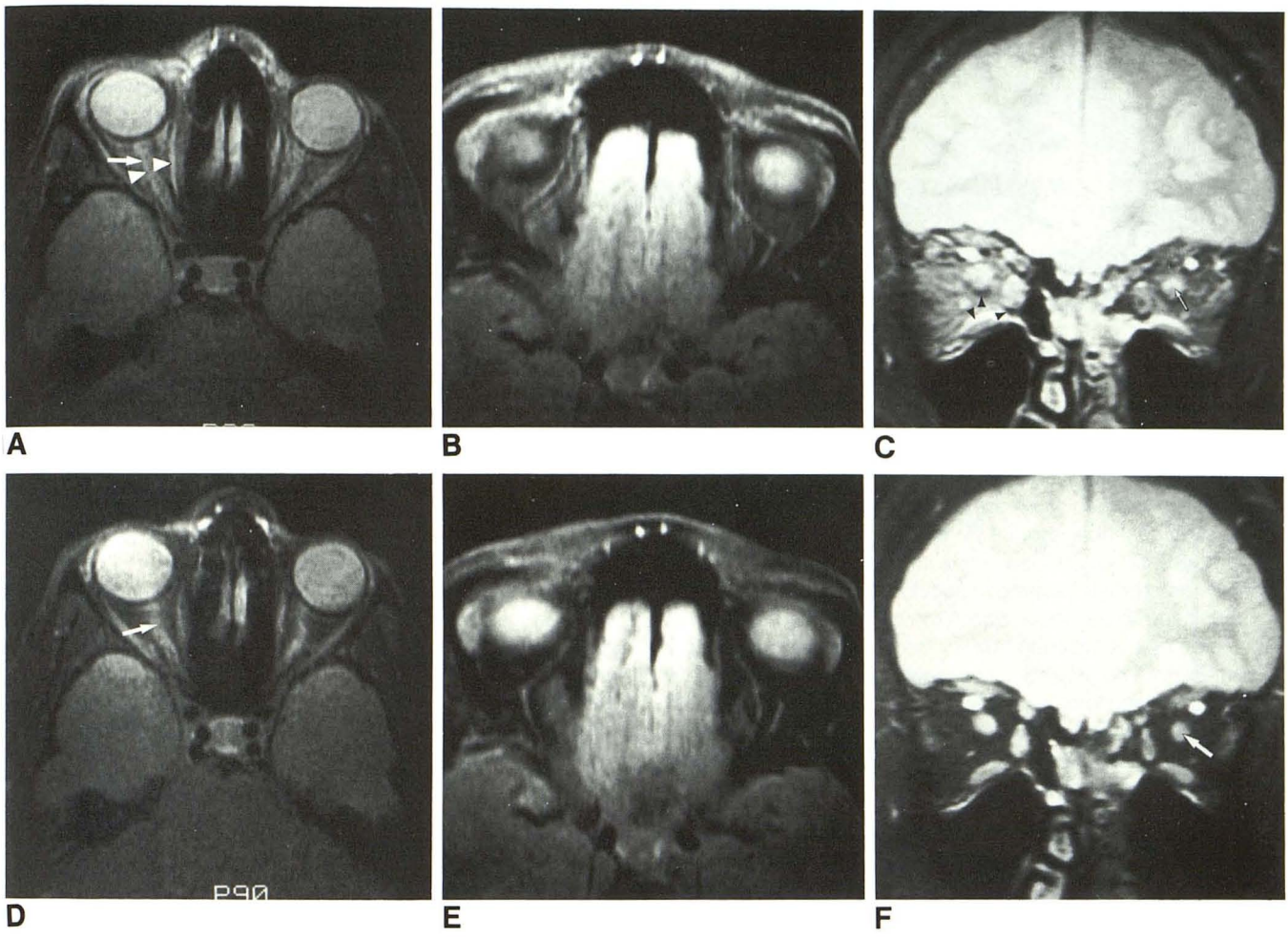

Fig. 4.—*A–F*, T2-weighted conventional axial (*A* and *B*) and coronal (*C*) images and fat-suppressed axial (*D* and *E*) and coronal (*F*) images (2000/60). Parameters are otherwise the same as those for Fig. 3. On conventional images, fat varied from isointense to slightly hypointense relative to optic nerve (*arrows* in *A, C, D,* and *F*). The chemical shift artifact (*arrowheads* in *A* and *C*), a dominant component of the conventional images, decreased with fat suppression. Although not appreciable on these images, CSF might be expected to contribute to signal surrounding optic nerve, creating an impression of greater optic nerve width on both the conventional and fat-suppressed images.

by the fat-suppression technique throughout the range of T1 to T2 weighting. The lacrimal gland received the highest score for this category. Only at the upper range of T2 weighting did conventional imaging provide acceptable lacrimal gland detail. The intracanalicular optic nerve and optic chiasm were also in this category. Several anatomic regions showed anatomic advantages by fat suppression, which were, however, dependent on relative T1-T2 weighting. For example, the posterior wall of the globe was thought to be demonstrated better by T1-weighted fat-suppression imaging. In contrast, the intraconal segment of the optic nerve and the extraocular muscles were considered to be imaged to advantage on more T2-weighted fat-suppressed images. Anterior chamber anatomy was judged to be less optimal on T1-weighted fat-suppressed images. Finally, fat suppression was rated strongly negative on all axial studies for demonstrating intraorbital venous structures. This was believed to be related in part to the filming technique, which resulted in visual "flare" from the dominating bright intensity of the venous structures.

Discussion

Fat-suppression imaging of the orbit has recently been shown to provide advantages in eliminating chemical shift artifact [5, 10] and is promising for lesion detection such as in optic neuritis [9]. Our results suggest that, in addition, fat-suppression techniques applied at specific combinations of TR and TE offer several potentially useful combinations of contrast that can improve anatomic detail and lesion contrast.

There are several problems observed in conventional orbital MR imaging that have possible solutions based on exploiting the weighting-dependent fat-suppression technique. Problems in orbital MR imaging related to the high lipid content include chemical shift misregistration artifact and contrast-

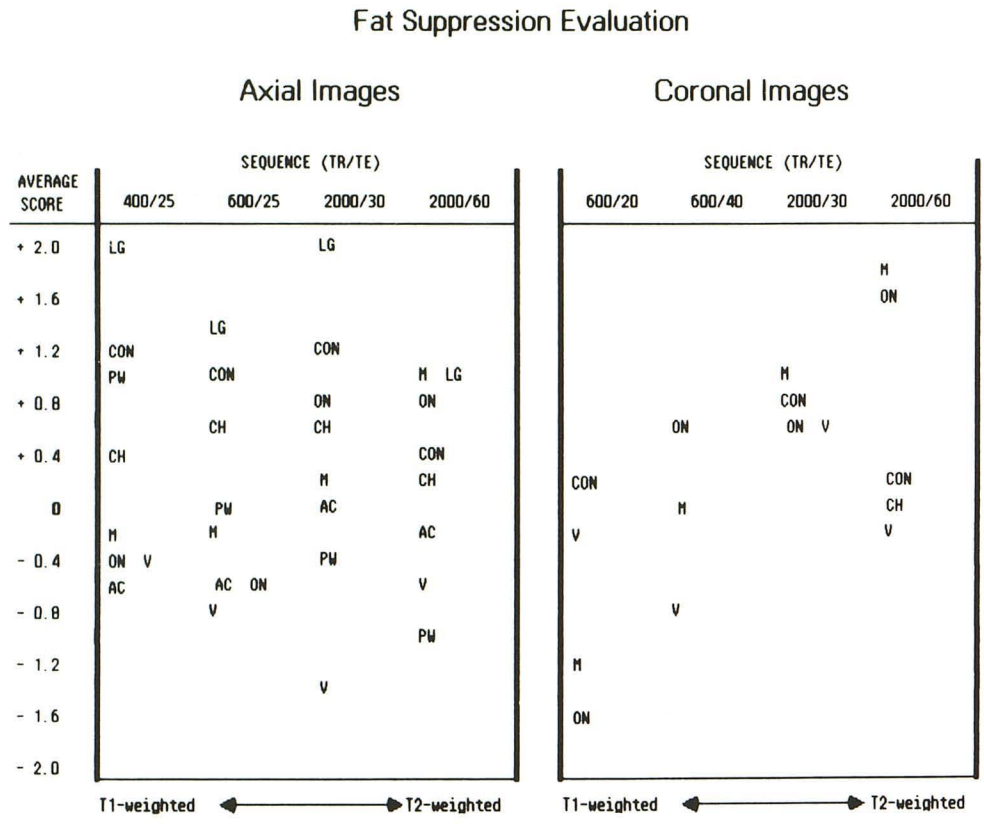

Fig. 5.—Average evaluation scores versus TR/TE for selected anatomic regions of interest. Positive or negative scores indicate favorable or unfavorable responses to fat-suppression images, respectively, relative to conventional images, based on review by five radiologists. Missing values are the result of exclusion of an anatomic region of interest from the image. LG = lacrimal gland; ON = optic nerve, intraconal segment; CON = optic nerve, canalicular segment; PW = posterior wall of globe including sclera, choroid, and retina; CH = optic chiasm; M = extraocular muscles; V = major intraorbital veins; AC = anterior chamber structures including lens, iris, ciliary body, and region of cornea.

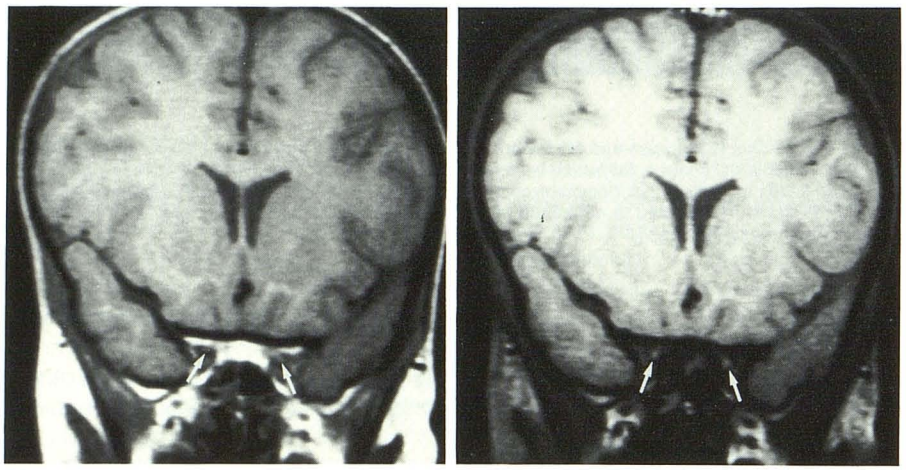

Fig. 6.—*A* and *B*, Conventional (*A*) and fat-suppressed (*B*) T1-weighted images of orbital apex–optic canal junction. Coronal images (800/25, 5 mm thick) obtained in a child with known optic chiasm glioma using standard head coil. In *A*, optic nerve (*arrows*) is not easily separable from surrounding high-intensity fat in marrow. By using fat suppression (*B*) normal-appearing optic nerve (*arrows*) is well contrasted with all adjacent structures and is easily photographed using a narrow window without interference from fat.

related limitations. Chemical shift misregistration artifact takes the form of high- and low-intensity bands that obscure detail, particularly affecting the optic nerve [5], and that also interfere with anatomic detail of the extraocular muscle margins and with the interface between sclera and retroorbital fat. These artifacts are not entirely eliminated with the Dixon method [5] or with chopper fat suppression, but they are decreased through all TR/TE combinations.

A potentially important contrast-related problem is the situation in which there are confounding combinations of adjacent signal intensities. This results, for example, in an illusion of a thick optic nerve caused by the visually dominating high-intensity fat on T1- and intermediate-weighted images, and a similar though probably less important effect on muscle (Fig. 2A). A more easily interpreted image is formed by using fat-suppression T1- (Fig. 2C) or intermediate-weighted sequences (2000/30) (Figs. 3D and 3F) in which the higher-intensity optic nerve, for example, is only surrounded by low-intensity structures (CSF, dura, and fat).

We have experienced several situations in which contrast is inadequate in the orbit. For example, the optic nerve and surrounding CSF may be nearly isointense with orbital fat on

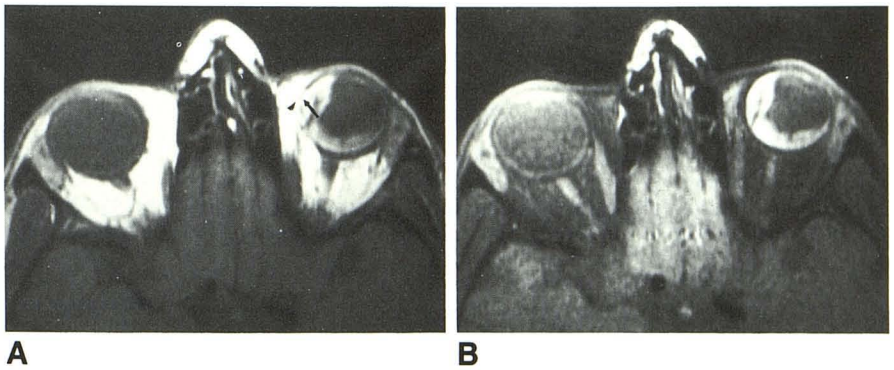

Fig. 7.—*A* and *B*, Conventional (*A*) and fat-suppressed (*B*) T1-weighted axial surface-coil images (500/25, 3 mm thick) in a patient with known uveal melanoma and retinal detachment.

***A*, Medial margins of lesion (*arrow*) are inseparable from medial orbital fat (*arrowhead*).**

***B*, Fat-suppression image shows sharply defined medial border owing to loss of interfering fat signal intensity.**

conventional T2-weighted images (Figs. 4A and 4C). The lacrimal gland is nearly isointense with adjacent orbital fat and fat within the medullary cavity of the adjacent bone (Fig. 4B). High-intensity signal originating from the marrow of the anterior clinoid processes or posterior ethmoid sinuses [12] may interfere with visualization of the optic nerve (Fig. 3A). The fat-suppression technique will increase contrast in all these cases. Miller et al. [9] have shown that fat suppression using STIR sequences is useful in demonstrating high-signal lesions of the optic nerve resulting from optic neuritis. Although not proved in this study, in theory, a fat-suppressed 2000/30 image should be ideal for demonstrating optic nerve high-signal lesions since the lesion should show positive contrast with all adjacent structures, including CSF.

Finally, fat may interfere with lesion detection when the orbit is filmed with a narrow window or beyond the gray scale [2]. Fat-suppression T1- or intermediate-weighted studies will not be dominated by bright intensities and consequently should be easier to film correctly.

Practical clinical application of fat-suppression techniques requires a minimal effect on acquisition or processing time, a user-friendly technique, and reasonable quality control with reproducible results. The chopper fat-suppression technique satisfies these criteria for orbital imaging. In comparison, the current standard, the original Dixon method [6], doubles acquisition time to acquire an in-phase image with water and fat magnetization parallel, and a second out-of-phase image with water and fat magnetization antiparallel. Additional post-processing is required in the Dixon method to generate so-called water-only images. Current software limitations on commercial MR instruments imply that images are added and subtracted after Fourier transform and after the magnitude calculation is performed. Even in an ideally homogeneous magnetic field, that approach results in fat suppression that is dependent on relative water and fat content in each voxel of the image [11]. The problem can be severe in areas where fat magnetization dominates the voxel, such as the orbit.

Chopper fat suppression further simplifies the Dixon method, and the nonlinearity problem is practically eliminated by using the averaging capability of the acquisition scheme. This method is sensitive to magnetic field inhomogeneities across the field of view of the image but field inhomogeneity is minimized by using the smaller field of view in orbit studies. The additional flexibility of a wide variety of TR and TE combinations should be advantageous compared with inversion recovery schemes, which are more sequence-limited.

Nevertheless, the chopper fat-suppression technique is not ideal. A minority of studies show inadequate fat suppression due to operator error in choice of prescan parameters. Similar to conventional techniques, proper surface-coil positioning is crucial to minimize signal inhomogeneity. It has been our impression that the chopper technique may be more sensitive to artifacts from patient motion than are conventional sequences. This is thought to be the result of a perception of increased noise in the image, which is in fact due to decreased signal (from lipid suppression). The overall decreased signal intensity in the orbit, and lower total signal-to-noise ratios in our early experience, resulted in an impression of less than optimal studies. However, with increasing experience and attention to proper prescan technique and coil placement, the lower overall orbital signal has not been a problem. Finally, there is always some loss of water signal intensity as a result of imperfect pulse parameters. Again, by proper selection of sequence parameters, including TR and TE combinations, that disadvantage seems to be adequately offset.

Fat-suppression techniques increase the number of sequence choices available for orbital MR imaging. On the basis of our preliminary experience, we believe that axial, fat-suppression, intermediate-weighted, 3-mm-thick images could replace conventional intermediate T2-weighted images. This sequence would provide visualization of the optic nerve separate from its sheath and improve visualization of the intracanalicular segment (Fig. 3D). Inflammatory lesions and demyelination, theoretically, should present as high-signal lesions on 2000/30 fat-suppressed images, well contrasted with optic nerve, CSF, and intraorbital fat. Preliminary studies using fat-suppression sequences in clinical practice show that the technique can be applied to clarify detail, particularly in the orbital apex or optic canal (Fig. 6), and to demonstrate the anatomic borders of lesions (Fig. 7).

In conclusion, the technical features of this recently introduced fat-suppression technique achieve the goal of clinical practicality. Fat-suppression techniques applied at the proper T1-T2 weighting should increase diagnostic information. Studies are currently in progress to determine the clinical utility of these techniques.

REFERENCES

1. Schenck JF, Hart HR, Foster TH, et al. Improved MR imaging of the orbit at 1.5 T with surface coils. *AJNR* **1985**;6:193–196
2. Atlas SW, Grossman RI, Savino PJ, et al. Surface-coil MR of orbital pseudotumor. *AJNR* **1987**;8:141–146
3. Bilaniuk LT, Schenck JF, Zimmerman RA, et al. Ocular and orbital lesions: surface coil MR imaging. *Radiology* **1985**;156:669–674
4. Sullivan JA, Harms SE. Surface-coil MR imaging of orbital neoplasms. *AJNR* **1986**;7:29–34
5. Daniels DL, Kneeland JB, Shimakawa AJ, et al. MR imaging of the optic nerve and sheath: correcting the chemical shift misregistration effect. *AJNR* **1986**;7:249–253
6. Dixon WT. Simple proton spectroscopic imaging. *Radiology* **1984**; 153:189–194
7. Atlas SW, Grossman RI, Axel L, et al. Orbital lesions: proton spectroscopic phase-dependent contrast MR imaging. *Radiology* **1987**;164:510–514
8. Bydder GM, Young IR. MR imaging: clinical use of the inversion recovery sequence. *J Comput Assist Tomogr* **1985**;9:659–675
9. Miller DH, Johnson G, McDonald WI, et al. Detection of optic nerve lesions in optic neuritis with magnetic resonance imaging. *Lancet* **1986**; 1(8496):1490–1491
10. Frahm J, Haase A, Hanicke W, Matthaei D, Bomsdorf H, Helzel T. Chemical shift selective MR imaging using a whole-body magnet. *Radiology* **1985**;156:441–444
11. Szumowski J, Plewes DB. Separation of lipid and water MR imaging signals by chopper averaging in the time domain. *Radiology* **1987**;165:247–250
12. Daniels DL, Herfkins R, Gager WE, et al. Magnetic resonance imaging of the optic nerves and chiasm. *Radiology* **1984**;152:79–83